


RESEARCH

Open Access



Epigenetic targeting of the ACE2 and NRP1 viral receptors limits SARS-CoV-2 infectivity

Maria Laura Saiz^{1†}, Marta L. De Diego^{2†}, Darío López-García², Viviana Corte-Iglesias¹, Aroa Baragaño Raneros¹, Ivan Astola^{3,4}, Victor Asensi⁵, Carlos López-Larrea^{1,6*} and Beatriz Suarez-Alvarez¹ 

Abstract

Background: SARS-CoV-2 uses the angiotensin-converting enzyme 2 (ACE2) and neuropilin-1 (NRP1) receptors for entry into cells, and the serine protease TMPRSS2 for S protein priming. Inhibition of protease activity or the engagement with ACE2 and NRP1 receptors has been shown to be an effective strategy for blocking infectivity and viral spreading. Valproic acid (VPA; 2-propylpentanoic acid) is an epigenetic drug approved for clinical use. It produces potent antiviral and anti-inflammatory effects through its function as a histone deacetylase (HDAC) inhibitor. Here, we propose VPA as a potential candidate to tackle COVID-19, in which rapid viral spread and replication, and hyperinflammation are crucial elements.

Results: We used diverse cell lines (HK-2, Huh-7, HUVEC, Caco-2, and BEAS-2B) to analyze the effect of VPA and other HDAC inhibitors on the expression of the ACE-2 and NRP-1 receptors and their ability to inhibit infectivity, viral production, and the inflammatory response. Treatment with VPA significantly reduced expression of the ACE2 and NRP1 host proteins in all cell lines through a mechanism mediated by its HDAC inhibitory activity. The effect is maintained after SARS-CoV-2 infection. Consequently, the treatment of cells with VPA before infection impairs production of SARS-CoV-2 infectious viruses, but not that of other ACE2- and NRP1-independent viruses (VSV and HCoV-229E). Moreover, the addition of VPA 1 h post-infection with SARS-CoV-2 reduces the production of infectious viruses in a dose-dependent manner without significantly modifying the genomic and subgenomic messenger RNAs (gRNA and sg mRNAs) or protein levels of N protein. The production of inflammatory cytokines (TNF- α and IL-6) induced by TNF- α and SARS-CoV-2 infection is diminished in the presence of VPA.

Conclusions: Our data showed that VPA blocks three essential processes determining the severity of COVID-19. It downregulates the expression of ACE2 and NRP1, reducing the infectivity of SARS-CoV-2; it decreases viral yields, probably because it affects virus budding or virions stability; and it dampens the triggered inflammatory response. Thus, administering VPA could be considered a safe treatment for COVID-19 patients until vaccines have been rolled out across the world.

Keywords: SARS-CoV-2, ACE2, HDAC, Epigenetic, NRP1, Valproic acid

Background

SARS-CoV-2 is the causal agent of the coronavirus-induced disease 2019 (COVID-19) pandemic, which had cost more than 3.4 million lives worldwide by the end of May 2021 [1]. The scenario has drastically changed since the start of the pandemic. Although several vaccines have been approved for use in humans [2–6], there are many concerns regarding their worldwide accessibility,

*Correspondence: inmuno@hca.es

[†]Maria Laura Saiz and Marta L. De Diego have contributed equally to this work

¹ Translational Immunology Laboratory, Instituto de Investigación Sanitaria del Principado de Asturias (ISPA), Oviedo, Spain
Full list of author information is available at the end of the article



© The Author(s) 2021. **Open Access** This article is licensed under a Creative Commons Attribution 4.0 International License, which permits use, sharing, adaptation, distribution and reproduction in any medium or format, as long as you give appropriate credit to the original author(s) and the source, provide a link to the Creative Commons licence, and indicate if changes were made. The images or other third party material in this article are included in the article's Creative Commons licence, unless indicated otherwise in a credit line to the material. If material is not included in the article's Creative Commons licence and your intended use is not permitted by statutory regulation or exceeds the permitted use, you will need to obtain permission directly from the copyright holder. To view a copy of this licence, visit <http://creativecommons.org/licenses/by/4.0/>. The Creative Commons Public Domain Dedication waiver (<http://creativecommons.org/publicdomain/zero/1.0/>) applies to the data made available in this article, unless otherwise stated in a credit line to the data.

long-term efficacy, and usefulness in preventing infection with emerging virus variants. Thus, new treatments are required to manage patients with severe symptoms and those who are more vulnerable to SARS-CoV-2 infection.

SARS-CoV-2 virus enters human cells by the recognition and binding of the spike (S) protein to several cellular receptors, the angiotensin-converting enzyme 2 (ACE2) receptor being the main protein mediating viral entry [7, 8]. Initially, the receptor-binding domain (RBD) of the S1 subunit of the S protein binds the ACE2 receptor, favoring attachment to the surface of target cells [9]. Then, S protein priming by various cellular proteases facilitates the entry and fusion of the viral envelope and cellular membranes. The protease furin cleaves the S protein at the S1/S2 interface, which is further primed by the serine protease TMPRSS2. Once cleaved, the C-end rule (CendR) motif is exposed and binds to the cell surface neuropilin 1 (NRP1), which acts as another attachment factor contributing to virus entry and tropism [10, 11]. The receptors, ACE2 and NRP1, are both expressed in many human tissues, most notably the lung, but also others such as the gastrointestinal tract, kidney, and endothelial cells of the blood vessels and microvasculature. NRP1 is also found in the olfactory epithelia, neurons, and immune cells and probably contributes to the multiple systemic effects of SARS-CoV-2 [12]. Inhibition of protease activity or the engagement with ACE2 and NRP1 receptors has been shown to be an effective strategy for blocking infectivity and viral spreading. Neutralizing antibodies raised against the S protein obtained from convalescent SARS-CoV-2 patients can block viral entry through ACE2 [13]. Thus, drugs aimed at reducing or inhibiting the expression of these receptors may help prevent cellular entry of the virus and reduce its transmission to neighbor cells once the infection has taken place, thereby limiting its spread.

Some SARS-CoV-2-infected patients (20–40%) develop acute respiratory distress syndrome (ARDS) leading, in most cases, to death from COVID-19. These patients show a strong inflammatory response, similar to that of cytokine release syndrome, and increased migration of neutrophils to the lung tissue triggered by the inflammatory mediators released from local immune, epithelial, and endothelial cells, such as TNF- α and IL-6 [14]. Therefore, the blockage of viral entry and reduction of the inflammatory response are the two main targets at which most treatments are aimed. Drugs such as hydroxychloroquine and remdesivir with direct antiviral effects [15–17] and drugs with immunomodulatory properties (dexamethasone, tocilizumab, etanercept, and anakinra) [18–22] are currently used to treat COVID-19 patients.

Valproic acid (VPA; 2-propylpentanoic acid) is a branched short-chain fatty acid approved as a

mood-stabilizing anticonvulsant and a broad-spectrum antiepileptic drug [23]. For more than 50 years, VPA has been used to treat epilepsy and bipolar disorders, and as migraine prophylaxis. More recent discoveries about VPA's function as an inhibitor of histone deacetylases (HDACs) have aroused new interest in this epigenetic inhibitor as a cancer treatment [24, 25]. Moreover, due to its low cost, favorable side effect profile, and the ease with which it crosses the blood brain barrier, VPA is an attractive candidate drug for a variety of possible indications. However, it is contraindicated in pregnancy due to the high risk of congenital malformations [26].

To date, several in vitro and animal studies have demonstrated the potent anti-inflammatory and antiviral effects of VPA, two of the key events in targeting severe COVID-19. As an HDAC inhibitor, VPA decreases the production of NF- κ B-induced proinflammatory cytokines such as TNF- α and IL-6, promotes the differentiation to Th2 and regulatory T cells, and modulates neutrophil migration and IFN- γ -activated macrophage response, among other activities [27–30]. Additionally, VPA has demonstrated direct antiviral activity against enveloped viruses such as vesicular stomatitis virus (VSV), Semliki forest virus (SFV), West Nile virus (WNV), vaccinia virus (VACV), and lymphocytic choriomeningitis virus (LCMV), by inducing the generation of highly unstable viral particles through its properties as a disruptor of lipid composition of cellular membranes [31, 32]. More recently, the antiviral efficacy of VPA against herpes simplex virus 1 (HSV-1) has been reported, showing that patients receiving VPA treatment had a lower risk of herpesvirus infection than those not treated with this compound [33].

Given the aforementioned effects, some letters and reviews have already championed the therapeutic potential of VPA for COVID-19 patients [34–36]. Nevertheless, so far, the actual mechanisms by which VPA could be useful in SARS-CoV-2 infection have not been addressed. Our results demonstrate that VPA not only reduces the expression of the S protein receptors, ACE2 and NRP1, but also blocks viral production, restricting viral spread between neighboring cells. Also, VPA acts as a potent immunosuppressor, reducing the production of proinflammatory cytokines. All these effects make VPA a suitable candidate for treating COVID-19 patients.

Results

VPA reduces ACE2 and NRP1 expression in cells from different tissues by an HDAC-dependent mechanism

Recent studies have yielded powerful evidence that angiotensin-converting enzyme 2 (ACE2) is the major cellular-entry receptor for the SARS-CoV-2 virus, and ACE2 expression may increase tissue susceptibility to

SARS-CoV-2 infection [37]. In fact, the different ACE2 levels in a variety of tissues and cell types indicate the specific vulnerability of each organ to the infection [38].

Here, we analyzed the effect of VPA on ACE2 expression in human cell lines of different origins (lung, kidney, primary endothelium, for BEAS-2B, HK-2, and HUVEC cells, respectively) and in two tumor-derived cell lines (hepatocarcinoma and colorectal carcinoma, for Huh-7 and Caco-2 cells, respectively). To this end, we treated cells for 24 h with a range of nontoxic VPA concentrations (1–8 mM), previously determined by Annexin V/7AAD assay (Additional file 1: Fig. S1) and quantified the transcriptional and protein levels of ACE2 expression. First, we confirmed that all untreated cells show a high level of expression of ACE2 (Fig. 1A, B). Treatment with VPA significantly decreased ACE2 expression at the mRNA (Fig. 1A) and protein (Fig. 1B) levels in a dose-dependent manner in all the analyzed cell lines. Furthermore, protein levels of ACE2 were almost fully inhibited at a dose of 8 mM (Fig. 1A, B). We further evaluated the effect of VPA on the expression of NRP1, an additional host factor that facilitates SARS-CoV-2 entry. Interestingly, similar results to those shown for ACE2 were observed. VPA drastically reduced the mRNA expression levels of NRP1 in a dose-dependent fashion, which was also correlated with a decrease at the protein level (Fig. 1C, D). However, the transcriptional levels of other genes such as *CTSL1* (endosomal cysteine protease Cathepsin L, used for SARS-CoV for S protein priming), *DPP4* (the primary receptor for MERS-CoV), and *RFX5* (transcription factor essential for MHC class II expression) in HK-2 and Huh-7 cells remain unchanged after VPA treatment (Additional file 2: Fig. S2) [13, 39, 40]. These results therefore indicate that VPA specifically interferes with the transcriptional regulation of ACE2 and NRP1 receptors, impairing their expression, independently of cell type or whether the cell lines are derived from tumors.

One of the most important characteristics of VPA is its ability to inhibit histone deacetylases (HDACs), thereby increasing the acetylation levels in lysine residues from histones and nonhistone proteins [41, 42]. VPA is known as a pan-inhibitor, since it inhibits class I (HDAC 1–3, and 8) and IIa (HDAC 4, 5, 7, and 9), but not those of other HDAC classes [43]. To address whether the effect of VPA on those receptors was mediated by this mechanism, we assayed the effect of other HDAC inhibitors on the ACE2 and NRP1 expression in HK-2 and Huh-7 cell

lines. Trichostatin A (TSA) is a reversible class I and II mammalian HDAC inhibitor, PCI-24781 specifically inhibits class I and IIb HDACs, TMP-195 is specific for class IIa HDACs and sirtinol was used as a specific SIRT1 and SIRT2 (class III HDACs) inhibitor. Data show that TSA and PCI-24781 lowered ACE2 and NRP1 mRNA and protein levels, while their levels were unchanged by TMP-195 and sirtinol treatments (Fig. 2 and Additional file 3: S3). These results validate the hypothesis that HDAC inhibition is the main mechanism involved in the decrease of ACE2 and NRP1 expression, likely due to the blockage of the class I HDACs that are inhibited by VPA, TSA, and PCI-24781.

Pretreatment with VPA inhibits SARS-CoV-2 infection

As VPA reduces the expression of ACE2 and NRP1, we analyzed whether the pretreatment of cells with VPA could affect SARS-CoV-2 infection. To this end, we used cell lines susceptible to SARS-CoV-2 infection, such as the tumor-derived Huh-7 cell line and the non-tumoral HK-2 cell line. Samples of Huh-7 and HK-2 cells were pretreated for 24 h with different concentrations of VPA (4–16 mM). After that, culture medium was replaced by fresh medium without VPA, and cells were then infected and virus titers analyzed 24 and 48 hpi (Fig. 3A). Previously, we evaluated the effect of VPA on cell proliferation of HK-2 and Huh-7 cells lines by MTT assay. It is of note that even at the highest concentration of VPA (16 mM), the inhibition of the proliferation was never greater than of 50% (Additional file 4: Fig. S4).

The results show that at 24 hpi, virus titers were more than 95% lower (22-fold difference, measured in PFU/ml) in HK-2 and more than 85% lower (sevenfold difference, measured in PFU/ml) in Huh-7 cells treated with the highest concentration of VPA (16 mM) compared with control cells (Fig. 3B and Additional file 5: Fig. S5). Similarly, at 48 hpi, virus titers in cells treated with the highest concentration of VPA were reduced by more than 97% and 85% (35- and eightfold decrease in HK-2 and Huh-7 cells, respectively, measured in PFU/ml) (Fig. 3B and Additional file 5: Fig. S5). Moreover, virus titers at 24 hpi, in HK-2 and Huh-7 cells pretreated with VPA at the highest concentration, compared with virus titers measured just after virus absorption (0 hpi), were only increased 2- and 15-fold, respectively, compared with the 50- and 100-fold increases in control cells, respectively. These results indicate that virus production was very limited,

(See figure on next page.)

Fig. 1 VPA downregulates ACE2 and NRP1 expression in cell lines from different sources. Human cell lines (BEAS-2B, HK-2, HUVEC, Caco-2, and Huh-7) were treated with different doses of VPA (1, 2, 4, and 8 mM) for 24 h. VPA was diluted in culture medium, which was also used as control. Expression of the ACE2 (a, b) and NRP1 (c, d) receptors was assayed by RT-qPCR (a, c) and western blot (WB) (b, d). *GADPH* and β -actin genes were used as endogenous controls to quantify mRNA and protein levels, respectively. Transcription levels were calculated by the $2^{-\Delta\text{CT}}$ method (ΔCT : CT gene test—CT endogenous control). Data are presented as the mean \pm SD of at least three independent experiments. * $p < 0.05$

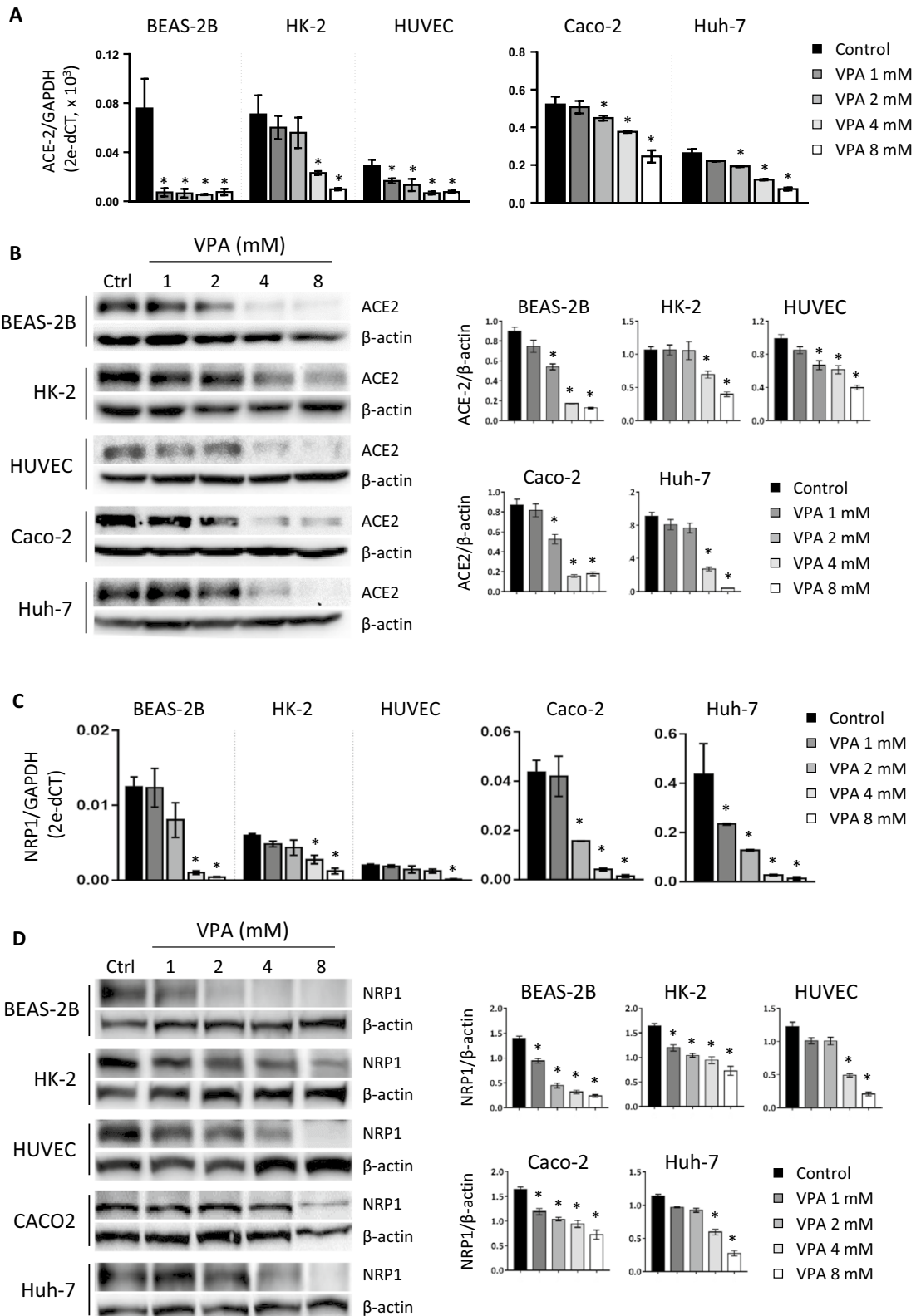


Fig. 1 (See legend on previous page.)

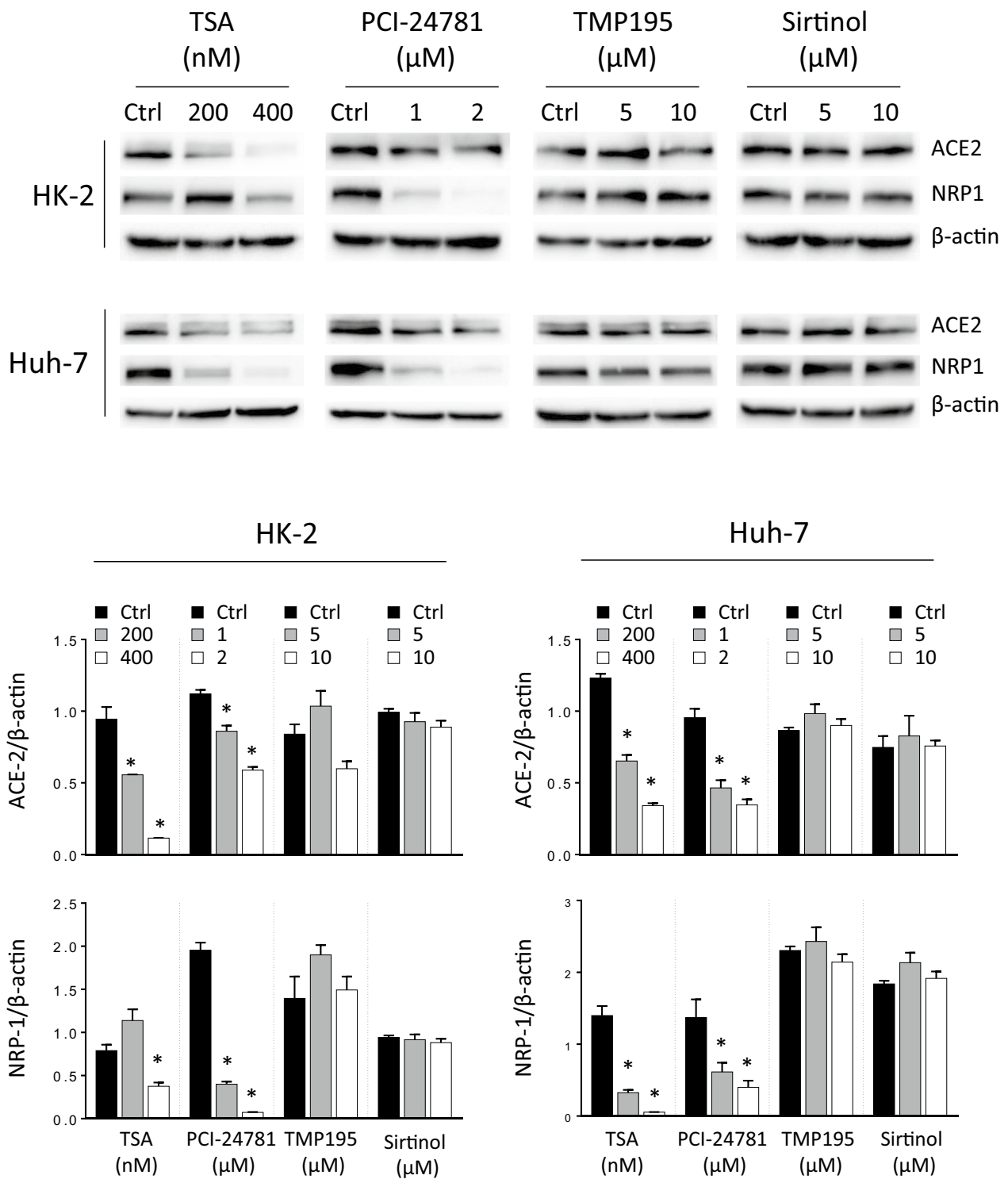
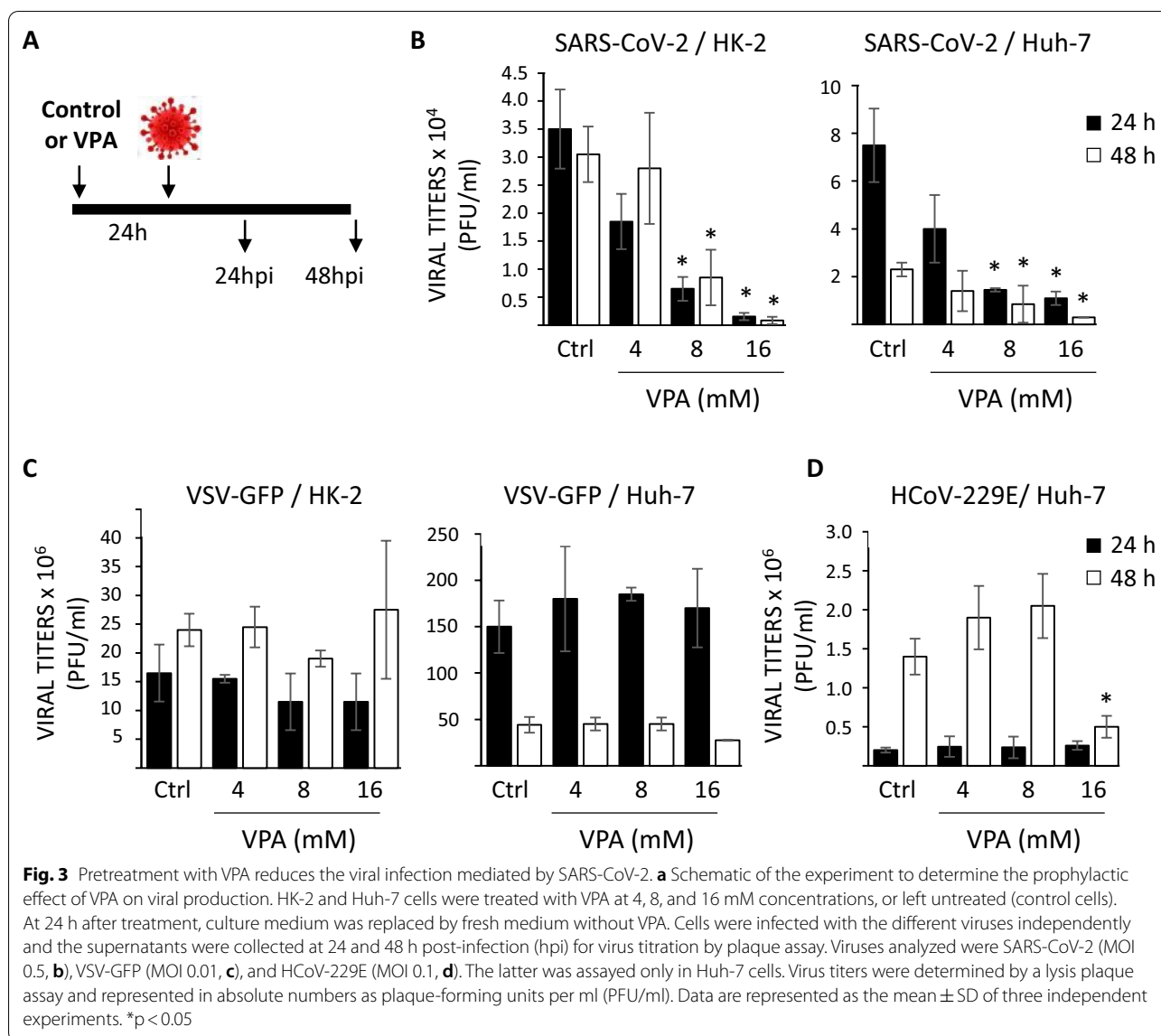


Fig. 2 Reduced expression of ACE2 and NRP1 is mediated by blocking histone deacetylases. HK-2 and Huh-7 cell lines were treated with different histone deacetylase (HDAC) inhibitors; trichostatin A (TSA, specific for class I and II HDACs, 200 and 400 nM), PCI-24781 (specific for class I and IIb HDACs, 1 and 2 μ M), TMP-195 (specific for class IIa HDACs, 5 and 10 μ M) and sirtinol (specific for SIRT1 and SIRT2, a class III HDAC, 5 and 10 μ M) for 24 h. All inhibitors were prepared in DMSO, which was also used as control. Expression of the ACE2 and NRP1 receptors was assayed by WB using β -actin as endogenous control. Data are presented as the mean \pm SD of at least three independent experiments. * $p < 0.05$



particularly in HK-2-treated cells (Additional file 5: Fig. S5). There was also a dose-dependent effect on the reduction of virus production (Fig. 3B and Additional file 5: Fig. S5), strongly suggesting that the pretreatment of cells with VPA reduces SARS-CoV-2 production. This effect is independent of the tumoral or non-tumoral origin of the cells.

To determine whether this effect also applies to other enveloped viruses, HK-2 and Huh-7 cells were infected with VSV-GFP and with another human coronavirus, the HCoV-229E (Fig. 3C, D). In contrast to VPA-treated SARS-CoV-2-infected cells, in which we observed a significant decrease in the yields of infectious viruses, no significant effect on the virus yields was detected in HK-2 and Huh-7 cells infected with VSV-GFP and

pretreated with VPA, even at the highest concentration, compared with the control cells (Fig. 3C, D). Moreover, regarding HCoV-229E infection experiments, only small (2.5-fold, measured in PFU/ml) differences were detected with the highest VPA concentration (16 mM) and only at 48 hpi (Fig. 3C, D) in Huh-7 cells. HK-2 cells were not susceptible to HCoV-229E infection (data not shown). Thus, these data show that pretreatment with VPA significantly reduced infection with SARS-CoV-2 but not with other viruses. The null or negligible effect observed with VSV-GFP and HCoV-229E, whose entry into mammalian cells is independent of those receptors, suggests that the outcome could be mediated, at least in part, by the effect of VPA on ACE2 and NRP1 expression.

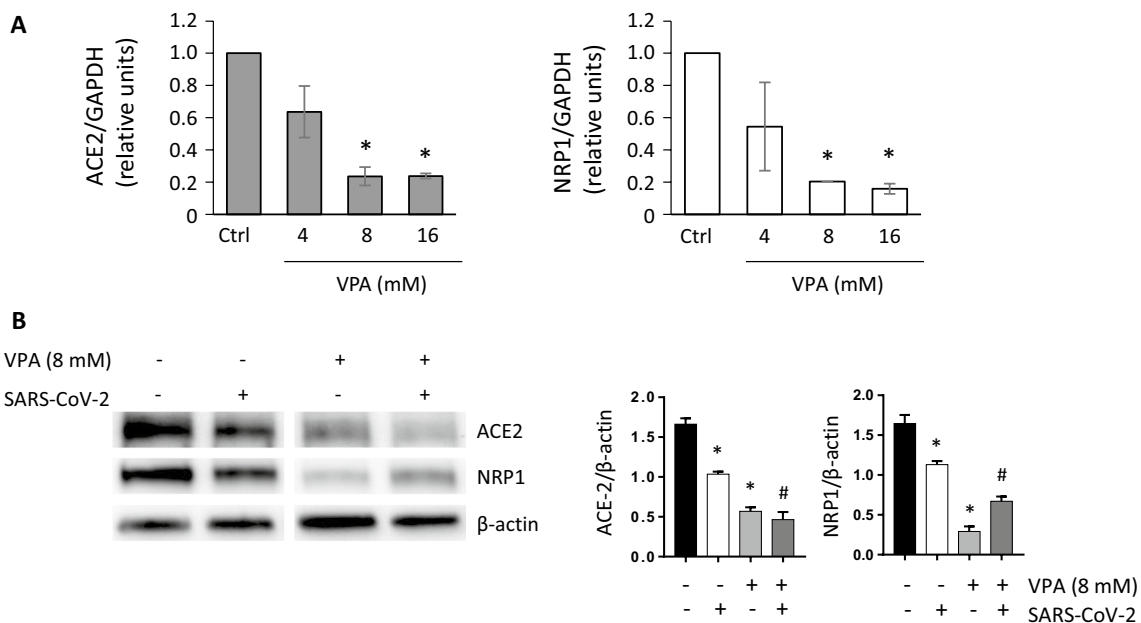


Fig. 4 VPA reduces ACE2 and NRP1 expression after SARS-CoV-2 infection. **a** Huh-7 cells were treated for 24 h with VPA at 4, 8, and 16 mM, or left untreated (control cells). They were then infected with SARS-CoV-2 (MOI 0.5) in the absence of VPA. The expression of ACE2 and NRP1 was analyzed by RT-qPCR at 24 hpi. GAPDH was used as the endogenous control and transcription levels were calculated by the $2^{-\Delta\text{CT}}$ method. The results are represented as levels relative to untreated (control) cells. **b** Huh-7 cells were treated with VPA (8 mM) for 24 h and further infected with SARS-CoV-2 (MOI 0.5) in the absence of VPA for additional 24 h. The levels of ACE2 and NRP1 proteins were assayed and quantified by WB, using β -actin as endogenous controls. All samples were analyzed at the same time and came from the same blot. Data are represented as the mean \pm SD of two independent experiments. * $p < 0.05$, compared with control; # $p < 0.05$, compared with SARS-CoV-2-infected cells

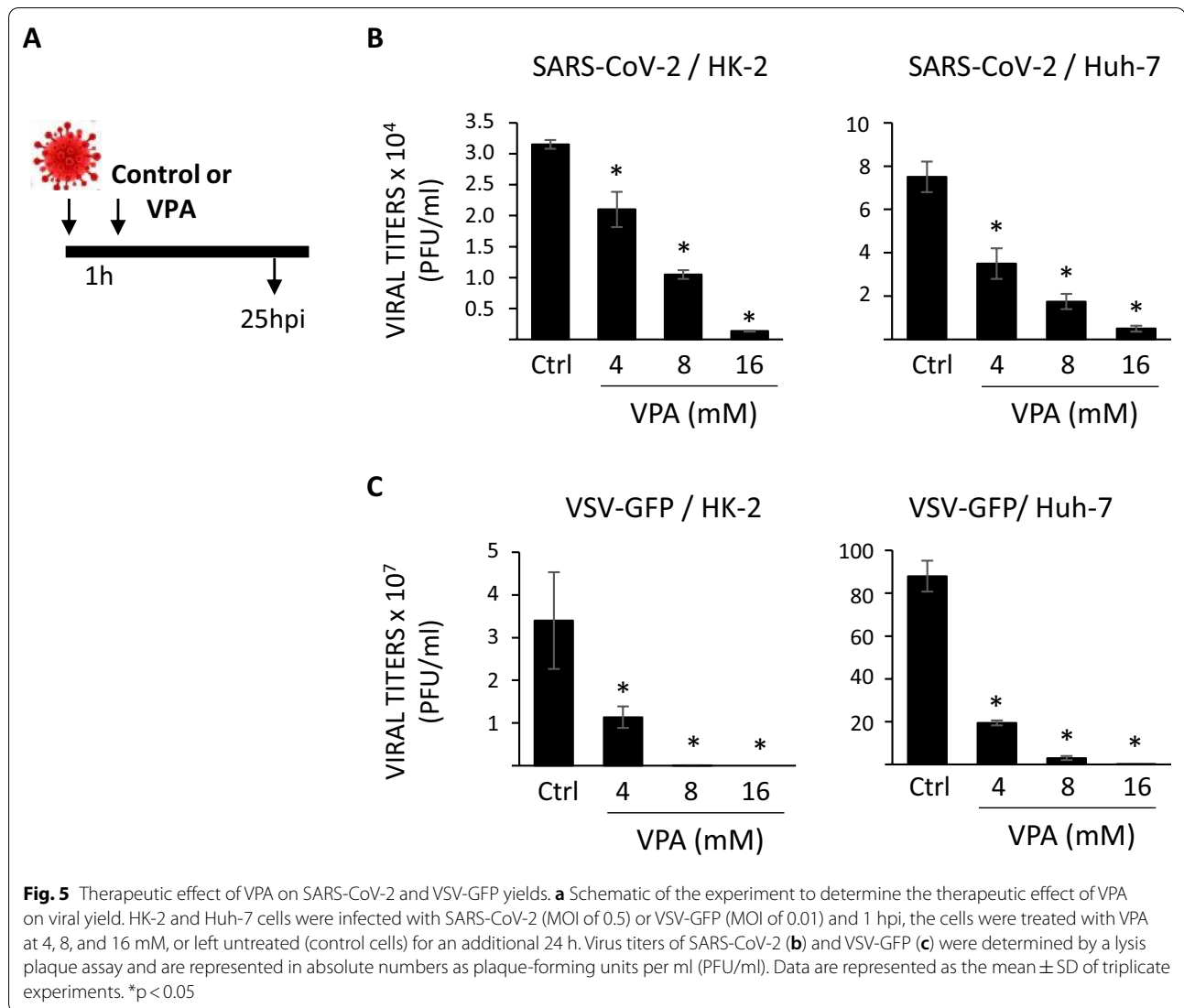
To obtain further evidence to support this hypothesis, samples of Huh-7 cells were pretreated for 24 h with different concentrations of VPA (4, 8, and 16 mM) and then infected with SARS-CoV-2 for 24 h. At the end of the experiment, ACE2 and NRP1 expression levels were quantified by RT-PCR and western blot. We observed that cells pretreated with VPA and additionally infected with SARS-CoV-2 maintained low levels of transcription for ACE2 and NRP1 compared with untreated control cells in a dose-dependent manner (Fig. 4A). We also confirmed that, although SARS-CoV-2 infection slightly downregulates ACE2 expression, as previously suggested [44], the effect of VPA (8 mM) on ACE2 and NRP1 protein levels was stronger and persisted at almost negligible levels 24 hpi (Fig. 4B). Thus, our findings could explain the potential effect of the pretreatment with VPA on the damaged infectivity of SARS-CoV-2.

Treatment with VPA post-infection reduces viral replication without affecting the synthesis of viral N protein

We wanted to evaluate the effect of VPA once SARS-CoV-2 infection has been established. To this end, HK-2 and Huh-7 cells were infected with SARS-CoV-2 or VSV-GFP and treated 1 hpi with different

concentrations (4–16 mM) of VPA. SARS-CoV-2 and VSV-GFP viral titers were measured at 24 hpi (Fig. 5A). The results showed that SARS-CoV-2 titers were more than 95% and 93% lower (23- and 15-fold, measured in PFU/ml) in HK-2 and Huh-7 cells, respectively, when the cells were treated with the highest VPA concentration compared with control cells (Fig. 5B and Additional file 6: Fig. S6). In this case, similar results were observed with the VSV-GFP virus, as VPA treatment after infection decreased titers by more than 99% (4,000,000- and 235,000-fold, measured in PFU/ml) in both cell lines at the highest VPA concentration, relative to control cells (Fig. 5C and Additional file 6: Fig. S6). Moreover, a dose-dependent effect on the reduction of infectious virus yields was observed under all conditions, and this effect applied both to tumoral- and non-tumoral-derived cell lines.

These findings suggested that VPA might inhibit post-entry steps of the life cycles of these viruses, reducing the quantity of infectious viruses. To rule out the possibility that the effect of VPA could be due to its ability to reduce cell growth, proliferation assays in HK-2 and Huh-7 cell lines were carried out in the presence of different concentrations of VPA at 24 h. The results showed that VPA reduced cell proliferation but never



reached $>50\%$ inhibition, even at the highest dose (Additional file 7: Fig. S7). Thus, these results suggest that the reduction in the viral titers induced by VPA is independent of its anti-proliferative effect.

To analyze whether VPA inhibits SARS-CoV-2 replication and transcription, HK-2 and Huh-7 cells were infected with SARS-CoV-2 for 1 h, then treated with VPA (4–16 mM). Total RNAs were extracted at 6 and 16 hpi, and the levels of genomic (g) (gRNA) and sub-genomic (sg) mRNAs (sg mRNAs) for the *N* gene were evaluated by RT-qPCR. No statistically significant differences were detected in control cells compared with VPA-treated cells, except for HK-2 cells, in which a slight decrease was observed at the highest VPA concentration (Fig. 6A). Likewise, when the *N* protein levels were detected in infected cells by western blot analysis, no difference was observed between the

control-infected cells and VPA-treated infected cells of the Huh-7 cell line, and there was only a negligible reduction with the 16 mM VPA dose in HK-2 cells (Fig. 6B). Taken together, these findings suggest that VPA inhibits the viral yield without interfering with the transcription and translation of viral proteins.

VPA reduces the inflammatory response triggered by TNF- α induction and virus infection

It has been extensively shown that SARS-CoV-2-induced pathology is due, at least in part, to an exacerbated inflammatory response [14, 45–47]. In addition, several studies have described how VPA can block the expression of inflammatory cytokines, including TNF- α and IL-6 [48, 49].

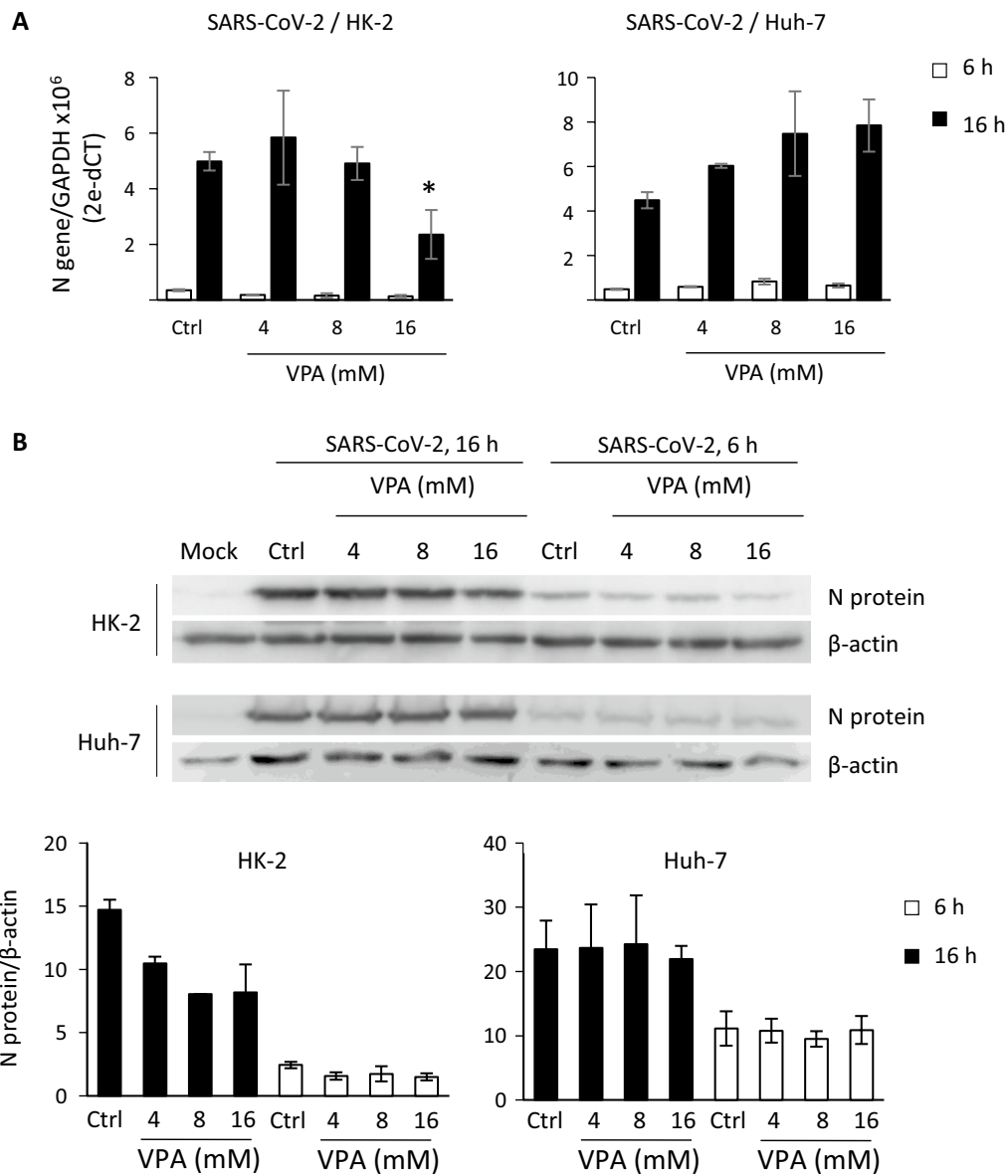
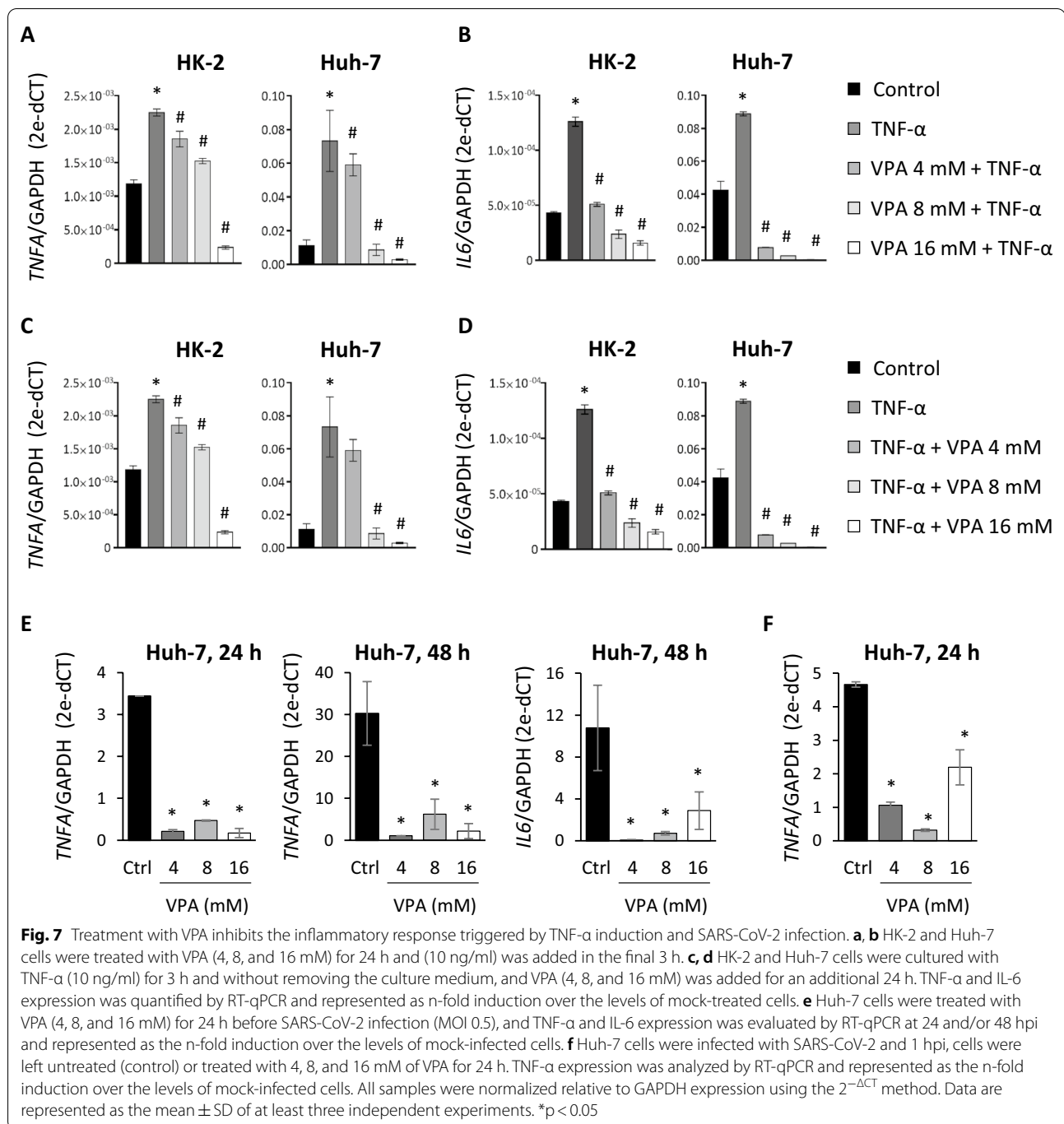


Fig. 6 VPA does not interfere with the synthesis of SARS-CoV-2 proteins. HK-2 and Huh-7 cells were infected with SARS-CoV-2 (MOI 0.5), and treated with VPA (4, 8, and 16 mM) 1 hpi. gRNA/sg mRNA expression levels (a) and protein levels (b) of protein N were analyzed at 6 and 16 hpi. *GADPH* (a) gene and β -actin (b) were used as endogenous controls for quantification of N gRNA/sg mRNA and protein levels. Data are presented as the mean \pm SD of at least three independent experiments. Mock; mock-infected cells (b). * $p < 0.05$

In accordance with this, we initially evaluated the effect of VPA in the expression of the pro-inflammatory cytokines, IL-6 and TNF- α , in HK-2 and Huh-7 cells, when the VPA was added before or after TNF- α induction. First, we checked that treatment with TNF- α (10 ng/ml) increased the expression of both cytokines under all the conditions analyzed (Fig. 7A–D). To measure the preventive effect of VPA, we cultured HK-2 and Huh-7 cells with different doses of VPA (4, 8, and 16 mM) for 24 h, adding TNF- α 3 h before

the end of the culture period. Expression levels of TNF- α and IL-6 were quantified by RT-qPCR. The results showed that VPA limited the increased expression of TNF- α and IL-6 in both cell lines in a dose-dependent way (Fig. 7A, B). The VPA effect was mainly observed in IL-6 expression, where the lowest dose of VPA assayed (4 mM) reduced its expression to levels seen in controls, at most (Fig. 7B). We also determined whether VPA had the same anti-inflammatory effect when it was added after TNF- α induction. Cell



lines were treated with TNF- α for 3 h and, without removing the culture medium, VPA was added for an additional 24 h. We again observed that the TNF- α and IL-6 mRNA levels were upregulated by TNF- α , although the increase was counteracted by the presence of VPA (Fig. 7C, D).

To establish whether VPA treatment has similar effects after SARS-CoV-2 infection, Huh-7 and HK-2 cells were treated with VPA for 24 h before infection. Cells were

then infected and the expression levels of TNF- α and IL-6 were evaluated by RT-qPCR at 24 and 48 hpi. The results showed that TNF- α expression levels were induced in control Huh-7 cells after 24 hpi (\pm threefold) but not in infected cells pretreated with VPA (Fig. 7E). These results were more evident at 48 hpi, at which time TNF- α expression is around 30 times higher in SARS-CoV-2-infected Huh-7 cells, whereas in VPA-pretreated cells its expression

had only increased 2- to fivefold (Fig. 7E). Similar results were observed in IL-6 expression, although in that case the induction was only detected at 48 hpi (Fig. 7E). Surprisingly, after SARS-CoV-2 infection, we could not detect the induction of TNF- α or IL-6 in HK-2 cells, even after 48 hpi (data not shown). In summary, VPA treatment could also prevent the inflammatory response triggered as a consequence of SARS-CoV-2 infection. In order to determine whether VPA could have a therapeutic effect and reduce the expression of pro-inflammatory cytokines when administered after SARS-CoV-2 infection, Huh-7 cells were infected and VPA was added 1 hpi for an additional 24 h. Once again, a decrease in TNF- α expression was observed for VPA-treated SARS-CoV-2-infected cells compared with untreated, infected cells (Fig. 7F). As reported above, IL-6 expression was not evaluated because the level of that cytokine had not increased 24 hpi.

Overall, these findings indicate that besides reducing the extent of production of infectious viruses, VPA also suppresses the expression of inflammatory cytokines after infection. This effect is probably not linked to the effect of VPA on limiting virus production since the same effect is observed by inducing the expression of inflammatory cytokines by TNF- α , in the absence of virus infection. This gives VPA an added value for controlling the exacerbated inflammatory response upon SARS-CoV-2 infection, which can lead to acute respiratory distress syndrome, and a worse prognosis for COVID-19.

Discussion

Infection by SARS-CoV-2 may cause patients to develop an exacerbated inflammatory response and extensive spread of the virus to multiple organs, leading to severe complications such as pneumonia and multiorgan dysfunction [50]. Here we show that VPA, a drug approved for the treatment of epilepsy, bipolar disorders, and migraines, can reduce the expression of the main cellular receptors of SARS-CoV-2, ACE2 and NRP1, in cell lines from a variety of human sources and thereby impair the spread of the virus to neighboring cells. Moreover, in SARS-CoV-2-infected cells, treatment with VPA reduces the production of infectious viruses without significantly modifying viral RNA and protein synthesis and, according to one of the most widespread effects described for VPA, this drug can also inhibit the production of the TNF- α and IL-6 proinflammatory cytokines triggered by SARS-CoV-2 infection.

Our results establish that ACE2 and NRP1 expression is regulated by epigenetic mechanisms. VPA specifically reduces the transcriptional levels of both SARS-CoV-2 receptors, an effect that is probably mediated by its activity as an HDAC inhibitor. Teodori et al. carried out a bioinformatic analysis to show that the HDAC pathway

is the key to the pathogenicity of SARS-CoV-2 [51]. They proposed that activation of AT1R (angiotensin II receptor type 1) by the excessive accumulation of angiotensin II (AngII) leads to the stimulation of HDACs that upregulate ACE2 expression. Moreover, the clinically used HDAC inhibitor, panobinostat, suppresses the expression of ACE2 in the gastric cancer cell line, KATOIII [52]. Given that observation and our own findings, the blockage of HDAC activity by VPA or other specific inhibitors reduces ACE2 expression. Additionally, the VPA-induced ACE2 downregulation was maintained even during SARS-CoV-2 infection. HDACs are normally associated with transcriptional repression, so their inhibition is usually associated with increased gene expression. However, transcriptional repression arising from inhibition of HDACs is much less well known. Recent reports have shown that HDACs could also positively regulate transcription by stimulating transcription elongation using mechanisms involving enhancer RNA synthesis and displacement of negative elongation factor (NELF) at promoters [53]. Other studies have demonstrated that HDAC inhibitors can repress gene transcription by blocking RNA polymerase II elongation in breast cancer, which preferentially acts on highly expressed genes as well as on high copy number genes [54]. Thus, the action of VPA on ACE2 expression could be mediated through the aforementioned mechanisms, by an indirect mechanism in which this inhibitor might modify the acetylation levels in the regulatory region of genes, or directly by acting on transcription factors that are involved in the transcriptional repression of ACE2. Whatever the explanation, these epigenetic-regulated mediators need to be identified.

An earlier study had shown that SIRT1, a class III HDAC, binds to the promoter region of ACE2, reducing its expression under cell stress [55]. The angiotensin II/AT1R axis plays a key role in the aging of the kidney increasing chronic inflammation and cell senescence. However, the angiotensin 1–7 (Ang 1–7)/Mas receptor (MasR) axis, mediated by the activation of ACE2, counterbalances that effect. Administration of the sirtuin inhibitor, resveratrol, to aged mice favors the enhancement of the Ang 1–7/MasR axis mediated by ACE2 exerting a protective effect [56]. By contrast, we observed that the growth of several cell lines under physiological conditions and in the presence of sirtinol (a specific SIRT1 and SIRT2 inhibitor) does not modify ACE2 expression. Therefore, the regulation mediated by sirtuins could be restricted by the cellular state, since sirtuins are known to be involved in stress responses [57, 58]. A recent study that aimed to evaluate the inflammatory response induced by SARS-CoV-2 in the heart found that BRD4, a member of the BET family of bromodomains, is

responsible for triggering cardiac injury and dysfunction [59]. Blockage of BRD4 action with epigenetic treatments reduces ACE2 expression and viral titers and protects against cardiac dysfunction in the K18-hACE2 mouse model.

The mechanisms of epigenetic regulation involved in NRP1 transcription are less well known, but butyrate, an HDAC inhibitor derived from dietary fiber, and trichostatin A (TSA) are known to downregulate NRP1 expression [60]. Butyrate diminishes the recruitment of Sp1 to the *NRP1* promoter in colorectal cancer, whereas the effect of TSA on NRP1 expression in endothelial cells is mediated by semaphorine III [61].

There is an established link between ACE2 deficiency, hyperinflammation, and SARS-CoV-2 infection [62]. ACE2 deficiency is associated with the clinical features, such as hypertension, diabetes, and cardiovascular disease that result in more severe COVID-19. The dysregulation between the AgII/AT1R and AT2R/Ang 1–7/MasX axes, favoring the latter, could give rise to an inflammatory state that could be blocked by the additional effect of VPA on the NF- κ B pathway.

One of the best known effects of VPA is its ability to attenuate inflammation. In COVID-19 patients, the hyperproduction of proinflammatory cytokines, such as IL-1, IL-6, IL-12, IFN- γ , and TNF- α , helps determine the severity of the disease [63]. Accordingly, many experimental treatments have been proposed with the aim of limiting the extent of induction of inflammatory cytokines after SARS-CoV-2 infection. In our model, VPA reduces the expression of the pro-inflammatory cytokines TNF- α and IL-6 even after SARS-CoV-2 infection, making VPA a promising candidate for the treatment of COVID-19 patients. Similar effects were observed in monocytes and macrophages activated with lipopolysaccharide and in a variety of mouse models of inflammation in which VPA suppresses the expression of inflammatory cytokines in a NF- κ B pathway-dependent manner [28, 48, 64]. VPA alters the acetylation of p65 by decreasing its DNA-binding affinity. Several studies have shown that acetylation and deacetylation of specific lysine residues in the p65 subunit regulate NF- κ B-mediated gene expression [65–68]. Changes in the acetylation dynamics in each of the seven acetylated lysines modulate the DNA binding, the assembly with I κ B α , the transcriptional activity of specific genes, and the length of the inflammatory response [69–71]. In this way, acetylation of K122 and K123 causes p65 to detach from the DNA and exit the cytoplasm, thereby ending the NF- κ B-mediated inflammatory response. HDAC3 is involved in reversing these processes by deacetylating specific lysine residues and, consequently, the activation of the inflammatory response. In fact, blockage of HDAC3 activity by

selective inhibitors produces an anti-inflammatory effect in inflammatory lung diseases and LPS-activated macrophages [72, 73]. VPA reverts the HDAC-3-mediated deacetylation of p65, attenuating the expression of specific inflammatory genes regulated by NF- κ B [49, 74].

In addition to VPA's role as an HDAC inhibitor, the drug has multiple effects and molecular targets, such as interfering with the metabolism of membrane lipids, which boosts expression of phosphatidylcholine pathway genes or reduces that of phosphatidylinositol [75, 76]. In this way, alterations in the host cell membrane could impair the assembly and production of some viruses. Vazquez-Calvo et al. [31] showed that the treatment of cells with VPA fully abolished the production of infectious envelope viruses but did not change the production of nonenveloped viruses. Surprisingly, the effect was maintained when VPA was added after infection. However, although VPA did not alter the number of budding viral particles, it produced particles that are more unstable in the infection medium. These results suggest that the antiviral potential of VPA could be mediated by the modifications in the cellular membrane of the host that use the envelope viruses to release new viral particles [32]. Furthermore, VPA diminishes the yields of infectious HSV-1 particles [77], and our results show that VPA not only decreases the viral infectivity of the enveloped SARS-CoV-2 virus by inhibiting ACE2 and NRP1 expression, but also reduces the generation of infectious SARS-CoV-2 particles without interfering with the synthesis of viral proteins. VPA also inhibits the production of particles of VSV, another envelope virus, corroborating its antiviral effect independently of ACE2. Recent studies have indicated the potential of additional epigenetic remodelers to block SARS-CoV-2 production. Resveratrol, whose multiple biological properties include being an activator of SIRT1, reduces the viral titers by 80% in *in vitro* cultures, although the underlying mechanisms are unclear [78, 79]. Taken together, the evidence demonstrates that epigenetic mechanisms can regulate all the key viral processes: entry, replication and transcription, and egress of new and stable viral particles. Therefore, these mechanisms, some of which we do not yet fully understand, are potentially useful in conjunction with clinically approved epigenetic drugs in the fight against SARS-CoV-2.

In summary, our study demonstrates that VPA, a drug commonly used in patients with epilepsy and bipolar disorders, can influence the infectivity of SARS-CoV-2 and can dampen the production of inflammatory cytokines. However, we cannot ignore the fact that all the studies have been done using cell models and that although we used cell lines of different origins (tumoral, non-tumoral, and primary cells), the susceptibility and tolerance to

diverse doses of VPA could vary. Therefore, further studies in preclinical models are needed to determine the minimal effective dose of VPA that not only inhibits the expression of SARS-CoV-2 receptors and inflammatory molecules, but also defines the therapeutic range over which it could be considered a potential antiviral drug. Additionally, large clinical studies evaluating the SARS-CoV-2 infection outcomes in VPA-treated patients for epilepsy treatment could help to determine the effectiveness within the therapeutic range currently used. An advantage is that VPA has not exhibited any adverse interactions with treatments currently used for COVID-19, such as hydroxychloroquine, lopanivir, and remdesivir [34], although clinical trials are needed to evaluate the safety and efficacy of such drug combinations.

Conclusions

After more than one year's experience of the SARS-CoV-2 pandemic, we know that a huge hyperinflammatory response is triggered in COVID-19 patients that contributes to a very poor disease prognosis, that the disease is more serious in patients with specific comorbidities (e.g., diabetes mellitus, obesity, and hypertension), and that there are currently no effective therapeutic treatments that limit the replication of the virus once infection has taken place. Here, we show that VPA interferes with two essential processes in the viral cycle: It can reduce the infectivity of SARS-CoV-2, through downregulation of its receptors ACE2 and NRP1, and decreases the viral yields, probably by modulating virus budding or by altering the composition of the envelope producing virions to greatly reduce its stability. We also corroborate the earlier finding that VPA blocks the expression of the NF- κ B-mediated inflammatory cytokines in the context of infection mediated by SARS-CoV-2. Thus, until everyone in the world is vaccinated, we will have to evaluate the effectiveness of new and current treatments of COVID-19 disease. In this context, epigenetic compounds such as VPA, which shows antiviral and immunomodulatory effects, represent promising candidates for use as COVID-19 treatments.

Methods

Cell lines, viruses, and reagents

Several cell lines were used. The African green monkey kidney-derived epithelial Vero E6 cells and the human hepatocellular carcinoma cell line, Huh-7, were kindly provided by Luis Enjuanes (Centro Nacional de Biotecnología-CSIC). The HK-2 human proximal tubular cell line (CRL-3216TM), human lung epithelial BEAS-2B cells (CRL-9609TM), Caco-2 human colorectal adenocarcinoma cell line (HTB-37), and primary human umbilical vein endothelial cells (HUVECs) (CRL-1730TM) were all

obtained from the American Type Culture collection. Huh-7, Vero E6, and Caco-2 cells were grown in Dulbecco's modified Eagle's medium (DMEM) (Gibco, Invitrogen, CA) supplemented with 25 mM HEPES and 10% fetal bovine serum (Fisher). HK-2 cell line was grown in RPMI-1640 medium (Gibco) supplemented with 10% fetal bovine serum (Fisher), 1% Insulin-transferrin-selenium (Gibco) and 36 mg/ml of hydrocortisone (Sigma-Aldrich). BEAS-2B was maintained in LHC-9 serum-free medium (Gibco) and HUVECs cultured in a mixture of DMEM and Ham's-F12 medium (1:1) supplemented with 10% fetal bovine serum (Fisher), 50 μ g/ml ECGS (Sigma) and 0.1 mg/ml heparin (Sigma). All media were further supplemented with 100 U/ml penicillin and 100 μ g/ml streptomycin (Gibco).

SARS-CoV-2, isolated in Vero E6 cells, originating from a nasal swab from a patient infected in Madrid, Spain (unpublished results), and human coronavirus-229E (HCoV-229E) were kindly provided by Luis Enjuanes (Centro Nacional de Biotecnología-CSIC). Vesicular stomatitis virus expressing green fluorescent protein (VSV-GFP) has been previously described [80].

Valproic acid sodium salt (VPA; Sigma) was dissolved directly in culture medium at the indicated concentrations. The HDAC inhibitors Trichostatin A (TSA), PCI-24781 (specific for class I and IIb HDACs), TMP-195 (specific for class IIa HDACs), and sirtinol (specific for SIRT1 and 2, class III HDACs), obtained from Selleckchem, were prepared in DMSO.

Virus infections

Confluent monolayers of Huh-7 and HK-2 cells (24-well-format plates) were treated for 24 h with VPA at 4, 8, and 16 mM concentrations to enable the analysis of the prophylactic effect of VPA. Cells were then infected with SARS-CoV-2 (multiplicity of infection, MOI, 0.5), VSV-GFP (MOI 0.01), and HCoV-229E (MOI 0.1) for 24 and 48 h in the absence of VPA. Cell culture media were collected at 24 and 48 h post-infection (hpi) and titrated in Vero E6 cells as described below.

Confluent monolayers of Huh-7 and HK-2 cells (24-well-format plates) were infected with SARS-CoV-2 (MOI, 0.5), VSV-GFP (MOI 0.01), and HCoV-229E (MOI 0.1) to analyze the therapeutic effect of VPA. VPA was added to the media at 4, 8, and 16 mM concentrations 1 hpi. Media were collected and titrated 24 hpi. Additionally, at 6 and 16 hpi, SARS-CoV-2-infected cells (MOI, 0.5) were collected and used for total RNA purification, and others were collected in RIPA buffer (Cell Signaling Technology) supplemented with a protease inhibitor cocktail (Merck Millipore, MA, USA), and the cell extracts used for western blot analysis.

Virus titrations

Vesicular stomatitis virus expressing green fluorescent protein (VSV-GFP) was titrated by plaque assay (plaque-forming units per milliliter, PFU/ml) in Vero E6 cells. Confluent cell monolayers (24-well format) were infected with tenfold serial dilutions for 1 h at 37 °C, overlaid with 0.7% agar, and incubated at 37 °C for 1 day. HCoV-229E was titrated by plaque assay in Huh-7 cells. Confluent cell monolayers (24-well format) were infected with tenfold serial dilutions for 1 h at 33 °C, overlaid with 0.7% agar, and incubated at 33 °C for 4 days. SARS-CoV-2 virus titrations were performed in Vero E6 cells grown in 24-well plates and infected with tenfold serial dilutions of the virus. After 1-h absorption, cells were overlaid with low electroendosmosis agarose (Pronadisa) and incubated for 3 days at 37 °C. For all virus titrations, cells were fixed with 10% formaldehyde in phosphate buffer saline (PBS) and permeabilized with 20% methanol. Viral plaques were visualized and counted using crystal violet.

Western blot

Total protein samples from untreated and VPA-treated cultured cells were isolated in RIPA buffer (Cell Signaling Technology) supplemented with a protease inhibitor cocktail (Merck Millipore, MA, USA) for 30 min on ice. Proteins were quantified using Bradford protein assay (Bio-Rad) and 20–50 µg per lane were separated on 10% polyacrylamide-SDS gels, blotted onto 0.45-µm Immobilon-E PVDF membranes (Merck Millipore, MA, USA), and detected by western blot analysis. The following primary antibodies were used: ACE-2 antibody-AC18F (NBP2-80035, Novus Biologicals, CO, USA), recombinant anti-NRP1 antibody [ERP3113] (ab81321, Abcam, UK), SARS-CoV-2-nucleocapsid protein antibody (GTX135357, GeneTex, CA, USA), and β-actin antibody (13E5; Cell Signaling, MA, USA). Secondary donkey anti-rabbit (406401, Biolegend) and goat anti-mouse (10799354, Invitrogen) antibodies conjugated with HRP were used. Immunoreactive bands were visualized using Immobilon Forte Western HRP substrate (Merck Millipore, MA, USA) and quantified with ImageJ version 1.53c software (NIH).

Gene expression studies

Total RNA from untreated or VPA- and TNF-α-treated cell lines was isolated using a GeneMATRIX Universal RNA purification kit (EURx, Poland) following the manufacturer's instructions. For virus infections, RNAs from mock-infected or infected cells were extracted using a total RNA extraction kit (Omega Bio-tek, GA, USA) following the manufacturer's recommendations. Purified RNA (1 µg) was reverse-transcribed to cDNA

using a high-capacity cDNA reverse-transcription kit (Applied Biosystems). Quantification was performed by reverse transcription–polymerase chain reaction (RT-PCR) using a TaqMan gene expression assay (Applied Biosystems) for the human *TNFA* (Hs00174128_m1), *IL6* (Hs00174131_m1), *ACE2* (Hs01085331_m1), and *GAPDH* (Hs02786624_g1) genes with TaqMan gene expression master mix (Applied Biosystems). Expression of the *NRP1*, *CTSL1*, *DPP4*, and *RFX5* genes was analyzed using TB Green Premix Ex Taq (Takara, Japan) and the following primers: *NRP1*: 5'-TTCAGGATC ACACAGGAGATGG-3' (sense) and 5'-TAAACCACA GGGCTCACCAG-3' (antisense); *CTSL1*: 5'-AGGCAT TTATTTTGGAGCCAG-3' (sense) and 5'-AATTCACA ATGGTTTCTCC-3' (antisense); *DPP4*: 5'-GAAGAG AGGATTCCAAACAAC-3' (sense) and 5'-CATTGT TCCAAACATATGCC-3' (antisense) and *RFX5*: 5'-CTG ATGCTAAGAGCCCCAAC-3' (sense) and 5'-TCAGTG TGCTCTCCAGGTG-3' (antisense). To analyze the expression of the nucleocapsid phosphoprotein (*N*) gene from SARS-CoV-2, the 5'-GCCTCTTCTCGTTCCTCA TCAC-3' (sense) and 5'-AGCAGCATCACCGCCATT G-3' (antisense) primers were used with the Power SYBR Green master mix (Thermo Fisher Scientific). In both cases, for *NRP1* and *N* genes, the *GAPDH* gene was used to normalize the data using the 5'-TGCCATGGGTGG AATCATATTGGA-3' (sense) and 5'-TCGGAGTCA ACGGATTTGGGTCGT-3' (antisense) primers.

Apoptosis and proliferation assays

To analyze cellular viability, apoptotic and dead cells were quantified using the FITC Annexin V apoptosis detection kit and 7-AAD (Biolegend), following the manufacturer's instructions. BEAS-2B, HK-2, Huh-7, Caco-2, and HUVEC cells were plated in 6-well plates at a seeding density of 3×10^6 cells/well and a range of concentrations of VPA (1, 2, 4, 8, and 16 mM) were added for 24 h. After that, cells were removed and stained using the FITC-Annexin V Apoptosis detection kit with 7AAD (Biolegend), following the manufacturer's instructions, and analyzed on a Gallios Flow Cytometer (Beckman Coulter, Inc.). Early apoptotic cells were considered as Annexin V + 7AAD- and late apoptotic/necrotic cells as Annexin V + 7AAD+.

The effect of VPA on cell proliferation was analyzed with an MTT (3-(4,5-dimethylthiazol-2-yl)-2,5-diphenyltetrazolium bromide) assay. Huh-7 and HK-2 cells were seeded at a density of 5×10^3 cells/well in 96-well plates at the same VPA concentrations, as described above, for 24 h. Depending on the experimental requirements, medium was then replaced, and cells were cultured for a further 24 or 48 h or kept unreplaced for direct analysis. During the final 4 h, 0.5 mg/ml of MTT substrate was added to the cell culture. After that, the

medium was removed, and formazan crystals were dissolved with DMSO. Absorbance at 570 nm was read by a spectrophotometer (Bio-Rad).

Data analysis

VPA-treated and VPA-untreated cells were compared by Student's unpaired-samples *t* test and the Mann–Whitney *U* test using SPSS Statistics for Windows, Version 20.0 (IBM Corp., Armonk, NY, USA). Data are represented as the mean and standard deviation (SD) of at least three independent experiments. Differences were considered statistically significant for values of $p < 0.05$.

Abbreviations

ACE2: Angiotensin-converting enzyme 2; AngII: Angiotensin II; ARDS: Acute respiratory syndrome; AT1R: Angiotensin II receptor type 1; COVID-19: Coronavirus-induced disease 2019; gRNA: Genomic messenger RNA; HCoV-229E: Human coronavirus 229E; HDAC: Histone deacetylase enzyme; hpi: Hours post-infection; HSV-1: Herpes simplex virus-1; MOI: Multiplicity of infection; NELF: Negative elongation factor; NRP1: Neuropilin-1; PFU: Plaque-forming units; sg mRNA: Subgenomic messenger RNA; TSA: Trichostatin A; VPA: Valproic acid; VSV: Vesicular stomatitis virus.

Supplementary Information

The online version contains supplementary material available at <https://doi.org/10.1186/s13148-021-01168-5>.

Additional file 1: Fig. S1. Effect of the treatment with VPA on cell viability of different cell lines. All cell lines (BEAS-2B, HK-2, Huh-7, CACO-2, and HUVeC) were treated with VPA (1, 2, 4, 8, and 16 mM) for 24 h. Control cells were untreated and only grown with culture medium. After that, cells were stained with annexin V-FITC and 7AAD and early apoptotic (annexin V-FITC + and 7AAD-) and late apoptotic / necrotic (annexin V-FITC + and 7AAD+) cells were quantified by flow cytometry. (A) Data are presented as the percentage of necrotic and apoptotic cells at 24 h post-treatment with VPA. (B) Representative dot-plots of Annexin V/7AAD for each cell line after 24 h of VPA treatment. Numbers in the lower and upper right quadrants show the percentage of early apoptotic and late apoptotic/necrotic cells, respectively.

Additional file 2: Fig. S2. Expression of the *CTSL1*, *DPP4*, and *RFX5* genes after VPA treatment in HK-2 and Huh-7 cell lines. HK-2 and Huh-7 cells were treated with different doses of VPA (1, 2, 4, and 8 mM) for 24 h or untreated (control). Expression of *CTSL1*, *DPP4* and *RFX5* genes was assayed by RT-qPCR and *GADPH* was used as endogenous controls to quantify mRNA levels. Transcription levels were calculated by the $2^{-\Delta\text{CT}}$ method (ΔCT : CT gene test—CT endogenous control). Data are presented as the mean \pm SD of two independent experiments.

Additional file 3: Fig. S3. Treatment with HDAC inhibitors reduces the transcriptional levels of ACE-2 and NRP1. HK-2 and Huh-7 cell lines were treated with different histone deacetylase (HDAC) inhibitors; trichostatin A (TSA, pan-HDAC, 200–400 nM), PCI-24781 (specific for class I and IIb HDACs, 1 and 2 μM), TMP-195 (specific for class IIa HDACs, 5 and 10 μM) and sirtinol (specific for SIRT1 and SIRT2, 5 and 10 μM) were used. All inhibitors were prepared in DMSO, which was also used as the control. Expression of the ACE2 and NRP1 receptors was assayed by RT-qPCR using *GADPH* gene as endogenous controls. Transcription levels were calculated by the $2^{-\Delta\text{CT}}$ method (ΔCT : CT gene test—CT endogenous control). Data are presented as the mean \pm SD of at least three independent experiments. * $p < 0.05$.

Additional file 4: Fig. S4. Effect of VPA pretreatment on cell proliferation of HK-2 and Huh-7 cell lines. HK-2 and Huh-7 cell lines were treated

with VPA (1, 2, 4, 8, and 16 mM) for 24 h. At each particular time, culture medium was replaced by fresh medium without VPA, and cells were grown for an additional 24 and 48 h. Control cells were untreated and only grown with culture medium. Cell proliferation was quantified by fluorometric MTT assay and data are shown as the percentage of cells compared with that of control cells, represented as the mean \pm SD of triplicate measures.

Additional file 5: Fig. S5. Effect of VPA pretreatment on SARS-CoV-2 infectivity. HK-2 and Huh-7 cells were treated during 24 h with VPA at 4, 8, and 16 mM, or left untreated (control cells). After 24 h, culture medium was replaced by fresh medium without VPA and cells were infected with SARS-CoV-2, VSV-GFP, or HCoV-229E, and virus titers were determined by plaque assay at 24 and 48 hpi, as in Fig. 3, and represented as the percentage of the titers compared with the titers measured in control cells. Data are represented as the mean \pm SD of absolute frequencies from triplicate measures. * $p < 0.05$ compared with control.

Additional file 6: Fig. S6. Therapeutic effect of VPA on viral yield after SARS-CoV-2 infection. HK-2 and Huh-7 cells were infected with SARS-CoV-2 (A) or with VSV-GFP (B), and 1 h after infection, cells were treated with VPA at 4, 8, and 16 mM, or left untreated (control cells). Virus titers were determined by plaque assay at 24 hpi, as in Fig. 5, and represented as the percentage of the titers compared with the titers measured in control cells. Data are represented as the mean \pm SD of absolute frequencies from triplicate measures. * $p < 0.05$.

Additional file 7: Fig. S7. Effect of VPA on cell proliferation of HK-2 and Huh-7 cell lines. HK-2 and Huh-7 cell lines were treated with VPA (1, 2, 4, 8, and 16 mM) for 24 h. Control cells were untreated and only grown with culture medium. Cell proliferation was quantified by fluorometric MTT assay and data are shown as the percentage of cells compared with control cells, represented as the mean \pm SD from triplicate measures.

Acknowledgements

We thank Luis Enjuanes and José M. Honrubia (Centro Nacional de Biotecnología-CSIC, Madrid, Spain) for kindly providing us with the SARS-CoV-2 sample analyzed in this study.

Authors' contributions

BSA, CLL, MLD, IA, and VA designed the research, analyzed the data, and supervised the production of the manuscript; BSA and MLD drafted and revised the manuscript. MLS, MLD, DLG, VCI, and ABR did the research and analyzed the data. MLS and MLD oversaw the methodology and analysis. All the authors read and approved the final version of the manuscript.

Funding

This study was supported by the Plan Nacional de I + D + I 2013–2016 ISCIII (Spanish Institute of Health Carlos III; Grant Numbers PI17/01244, PI20/00639, and PI19/00184), the Spanish National Research Council (CSIC, COVID-19 INMUNGEN Project, Reference 202020E086) to MLD, and the Community of Madrid, Spain (Grant Reference 2017-T1/BMD-5155) to MLD. D.L.G. received a JAE-INTRO 2020 Fellowship from the Spanish National Research Council (CSIC, JAEINT-20-01805).

Availability of data and materials

All data generated or analyzed during this study are included in this published article and its supplementary information files.

Declarations

Ethics approval and consent to participate

Not applicable.

Consent for publication

Not applicable.

Competing interests

The authors declare that they have no competing interests.

Author details

¹Translational Immunology Laboratory, Instituto de Investigación Sanitaria del Principado de Asturias (ISPA), Oviedo, Spain. ²Department of Molecular and Cellular Biology, Centro Nacional de Biotecnología (CNB-CSIC), Madrid, Spain. ³Intensive Care Department, Hospital Universitario Central de Asturias, Oviedo, Spain. ⁴Translational Microbiology Research Group, Instituto de Investigación Sanitaria del Principado de Asturias (ISPA), Oviedo, Spain. ⁵Infectious Diseases Unit, Translational Research in Infectious Diseases Group, Hospital Universitario Central de Asturias, Instituto de Investigación Sanitaria del Principado de Asturias (ISPA), Oviedo, Spain. ⁶Department of Immunology, Hospital Universitario Central De Asturias, Oviedo, Spain.

Received: 2 July 2021 Accepted: 8 September 2021
Published online: 11 October 2021

References

- World Health Organization. WHO Coronavirus (COVID-19) Dashboard. <https://covid19.who.int>. Accessed 27 May 2021.
- Polack FP, Thomas SJ, Kitchin N, Absalon J, Gurtman A, Lockhart S, et al. Safety and efficacy of the BNT162b2 mRNA Covid-19 vaccine. *N Engl J Med*. 2020;383(27):2603–15. <https://doi.org/10.1056/NEJMoa2034577>.
- Anderson EJ, Roupael NG, Widge AT, Jackson LA, Roberts PC, Makhene M, et al. Safety and immunogenicity of SARS-CoV-2 mRNA-1273 vaccine in older adults. *N Engl J Med*. 2020;383(25):2427–38. <https://doi.org/10.1056/NEJMoa2028436>.
- Ramasamy MN, Minassian AM, Ewer KJ, Flaxman AL, Folegatti PM, Owens DR, et al. Safety and immunogenicity of ChAdOx1 nCoV-19 vaccine administered in a prime-boost regimen in young and old adults (COV002): a single-blind, randomised, controlled, phase 2/3 trial. *Lancet*. 2021;396(10267):1979–93. [https://doi.org/10.1016/S0140-6736\(20\)32466-1](https://doi.org/10.1016/S0140-6736(20)32466-1).
- Stephenson KE, Le Gars M, Sadoff J, de Groot AM, Heerwegh D, Truysers C, et al. Immunogenicity of the Ad26COV2S vaccine for COVID-19. *JAMA*. 2021;325(15):1535–44. <https://doi.org/10.1001/jama.2021.3645>.
- Sadoff J, Le Gars M, Shukarev G, Heerwegh D, Truysers C, de Groot AM, et al. Interim results of a phase 1–2a trial of Ad26COV2S covid-19 vaccine. *N Engl J Med*. 2021;384(19):1824–35. <https://doi.org/10.1056/NEJMo a2034201>.
- Shang J, Wan Y, Luo C, Ye G, Geng Q, Auerbach A, et al. Cell entry mechanisms of SARS-CoV-2. *Proc Natl Acad Sci USA*. 2020;117(21):11727–34. <https://doi.org/10.1073/pnas.2003138117>.
- Zhou P, Yang XL, Wang XG, Hu B, Zhang L, Zhang W, et al. A pneumonia outbreak associated with a new coronavirus of probable bat origin. *Nature*. 2020;579(7798):270–3. <https://doi.org/10.1038/s41586-020-2012-7>.
- Ou X, Liu Y, Lei X, Li P, Mi D, Ren L, et al. Characterization of spike glycoprotein of SARS-CoV-2 on virus entry and its immune cross-reactivity with SARS-CoV. *Nat Commun*. 2020;11(1):1620. <https://doi.org/10.1038/s41467-020-15562-9>.
- Cantuti-Castelvetri L, Ojha R, Pedro L, Djannatian M, Franz J, Kuivaneen S, et al. Neuropilin-1 facilitates SARS-CoV-2 cell entry and infectivity. *Science*. 2020;370(6518):856–60. <https://doi.org/10.1126/science.abd2985>.
- Daly JL, Simonetti B, Klein K, Chen K, Williamson MK, Antón-Plágaro C, et al. Neuropilin-1 is a host factor for SARS-CoV-2 infection. *Science*. 2020;370(6518):861–5. <https://doi.org/10.1126/science.abd3072>.
- Mayi BS, Leibowitz JA, Woods AT, Ammon KA, Liu AE, Raja A. The role of Neuropilin-1 in COVID-19. *PLoS Pathog*. 2021;17(1):e1009153. <https://doi.org/10.1371/journal.ppat.1009153>.
- Hoffmann M, Kleine-Weber H, Schroeder S, Krüger N, Herrler ES, et al. SARS-CoV-2 cell entry depends on ACE2 and TMPRSS2 and is blocked by a clinically proven protease inhibitor. *Cell*. 2020;181(2):271–2808. <https://doi.org/10.1016/j.cell.2020.02.052>.
- Mehta P, McAuley DF, Brown M, Sanchez E, Tattersall RS, Manson JJ. COVID-19: consider cytokine storm syndromes and immunosuppression. *Lancet*. 2020;395(10229):1033–4. [https://doi.org/10.1016/S0140-6736\(20\)30628-0](https://doi.org/10.1016/S0140-6736(20)30628-0).
- Wang M, Cao R, Zhang L, Yang X, Liu J, Xu M, et al. Remdesivir and chloroquine effectively inhibit the recently emerged novel coronavirus (2019-nCoV) in vitro. *Cell Res*. 2020;30(3):269–71. <https://doi.org/10.1038/s41422-020-0282-0>.
- Wang Y, Zhang D, Du G, Du R, Zhao J, Jin Y, et al. Remdesivir in adults with severe COVID-19: a randomised, double-blind, placebo-controlled, multicentre trial. *Lancet*. 2020;395(10236):1569–78. [https://doi.org/10.1016/S0140-6736\(20\)31022-9](https://doi.org/10.1016/S0140-6736(20)31022-9).
- Young B, Tan TT, Leo YS. The place for remdesivir in COVID-19 treatment. *Lancet Infect Dis*. 2021;21(1):20–1. [https://doi.org/10.1016/S1473-3099\(20\)30911-7](https://doi.org/10.1016/S1473-3099(20)30911-7).
- Ledford H. Coronavirus breakthrough: dexamethasone is first drug shown to save lives. *Nature*. 2020;582(7813):469. <https://doi.org/10.1038/d41586-020-01824-5>.
- Xu X, Han M, Li T, Sun W, Wang D, Fu B, et al. Effective treatment of severe COVID-19 patients with tocilizumab. *Proc Natl Acad Sci USA*. 2020;117(20):10970–5. <https://doi.org/10.1073/pnas.2005615117>.
- Duret PM, Sebbag E, Mallick A, Gravier S, Spielmann L, Messer L. Recovery from COVID-19 in a patient with spondyloarthritis treated with TNF-alpha inhibitor etanercept. *Ann Rheum Dis*. 2020;79(9):1251–2. <https://doi.org/10.1136/annrheumdis-2020-217362>.
- Cavalli G, De Luca G, Campochiaro C, Della-Torre E, Ripa M, Canetti D, et al. Interleukin-1 blockade with high-dose anakinra in patients with COVID-19, acute respiratory distress syndrome, and hyperinflammation: a retrospective cohort study. *Lancet Rheumatol*. 2020;2(6):e325–31. [https://doi.org/10.1016/S2665-9913\(20\)30127-2](https://doi.org/10.1016/S2665-9913(20)30127-2).
- Putman M, Chock YPE, Tam H, Kim AHJ, Sattui SE, Berenbaum F, et al. Anti-rheumatic disease therapies for the treatment of COVID-19: a systematic review and meta-analysis. *Arthritis Rheumatol*. 2021;73(1):36–47. <https://doi.org/10.1002/art.41469>.
- Tomson T, Battino D, Perucca E. The remarkable story of valproic acid. *Lancet Neurol*. 2016;15(2):141. [https://doi.org/10.1016/S1474-4422\(15\)00398-1](https://doi.org/10.1016/S1474-4422(15)00398-1).
- Lübbert M, Grishina O, Schmoor C, Schlenk RF, Jost E, Crysandt M, et al. Valproate and retinoic acid in combination with decitabine in elderly nonfit patients with acute myeloid leukemia: results of a multicenter, randomized, 2 2. Phase II Trial *J Clin Oncol*. 2020;38(3):257–70. <https://doi.org/10.1200/JCO.19.01053>.
- Caponigro F, Di Gennaro E, Ionna F, Longo F, Aversa C, Pavone E, et al. Phase II clinical study of valproic acid plus cisplatin and cetuximab in recurrent and/or metastatic squamous cell carcinoma of Head and Neck-V-CHANCE trial. *BMC Cancer*. 2016;16(1):918. <https://doi.org/10.1186/s12885-016-2957-y>.
- Robert E, Guibaud P. Maternal valproic acid and congenital neural tube defects. *Lancet*. 1982;2(8304):937. [https://doi.org/10.1016/s0140-6736\(82\)90908-4](https://doi.org/10.1016/s0140-6736(82)90908-4).
- Delgado FG, Cárdenas P, Castellanos JE. Valproic acid downregulates cytokine expression in human macrophages infected with dengue virus. *Diseases*. 2018;6(3):59. <https://doi.org/10.3390/diseases6030059>.
- Leu SJ, Yang YY, Liu HC, Cheng CY, Wu YC, Huang MH, et al. Valproic acid and lithium mediate anti-inflammatory effects by differentially modulating dendritic cell differentiation and function. *J Cell Physiol*. 2017;232(5):1176–86. <https://doi.org/10.1002/jcp.25604>.
- Saouaf SJ, Li B, Zhang G, Shen Y, Furuuchi N, Hancock WW, Greene MI. Deacetylase inhibition increases regulatory T cell function and decreases incidence and severity of collagen-induced arthritis. *Exp Mol Pathol*. 2009;87(2):99–1043. <https://doi.org/10.1016/j.yexmp.2009.06.003>.
- Nieto-Patlán E, Serafin-Lopez J, Wong-Baeza I, Pérez-Tapia SM, Cobos-Marín L, Estrada-Parra S, et al. Valproic acid promotes a decrease in mycobacterial survival by enhancing nitric oxide production in macrophages stimulated with IFN-gamma. *Tuberculosis (Edinb)*. 2019;114:123. <https://doi.org/10.1016/j.tube.2018.12.007>.
- Vázquez-Calvo A, Saiz JC, Sobrino F, Martín-Acebes MA. Inhibition of enveloped virus infection of cultured cells by valproic acid. *J Virol*. 2011;85(3):1267–74. <https://doi.org/10.1128/JVI.01717-10>.
- Vázquez-Calvo A, Martín-Acebes MA, Saiz JC, Ngo N, Sobrino F, de la Torre JC. Inhibition of multiplication of the prototypic arenavirus LCMV by valproic acid. *Antiviral Res*. 2013;99(2):172–9. <https://doi.org/10.1016/j.antiviral.2013.05.012>.
- Gil M, González-González R, Vázquez-Calvo A, Álvarez-Gutiérrez A, Martín-Acebes MA, Praena B, et al. Clinical infections by herpesviruses in patients treated with valproic acid: a nested case-control study in the Spanish

- primary care database, BIFAP. *J Clin Med*. 2019;8(9):1442. <https://doi.org/10.3390/jcm8091442>.
34. Unal G, Turan B, Balcioglu YH. Immunopharmacological management of COVID-19: Potential therapeutic role of valproic acid. *Med Hypotheses*. 2020;143:109891. <https://doi.org/10.1016/j.mehy.2020.109891>.
 35. Pitt B, Sutton NR, Wang Z, Goonewardena SN, Holinstat M. Potential repurposing of the HDAC inhibitor valproic acid for patients with COVID-19. *Eur J Pharmacol*. 2021;898:173988. <https://doi.org/10.1016/j.ejphar.2021.173988>.
 36. Naasani I. COMPARE analysis, a bioinformatic approach to accelerate drug repurposing against Covid-19 and other emerging epidemics. *SLAS Discov*. 2021;26(3):345–51. <https://doi.org/10.1177/2472555220975672>.
 37. Beyerstedt S, Casaro EB, Rangel EB. COVID-19: angiotensin-converting enzyme 2 (ACE2) expression and tissue susceptibility to SARS-CoV-2 infection. *Eur J Clin Microbiol Infect Dis*. 2021. <https://doi.org/10.1007/s10096-020-04138-6>.
 38. Zou X, Chen K, Zou J, Han P, Hao J, Han Z. Single-cell RNA-seq data analysis on the receptor ACE2 expression reveals the potential risk of different human organs vulnerable to 2019-nCoV infection. *Front Med*. 2020;14(2):185–92. <https://doi.org/10.1007/s11684-020-0754-0>.
 39. Li Y, Zhang Z, Yang L, Lian X, Xie Y, Li S, et al. The MERS-CoV receptor DPP4 as a candidate binding target of the SARS-CoV-2 spike. *iScience*. 2020;23(8):101400. <https://doi.org/10.1016/j.isci.2020.101400>.
 40. Wu X, Fan Z, Chen M, Chen Y, Rong D, Cui Z, et al. Forkhead transcription factor FOXO3a mediates interferon- γ -induced MHC II transcription in macrophages. *Immunology*. 2019;158(4):304–13. <https://doi.org/10.1111/imm.13116>.
 41. Phiel CJ, Zhang F, Huang EY, Guenther MG, Lazar MA, Klein PS. Histone deacetylase is a direct target of valproic acid, a potent anticonvulsant, mood stabilizer, and teratogen. *J Biol Chem*. 2001;276(39):36734–41. <https://doi.org/10.1074/jbc.M101287200>.
 42. Gurvich N, Tsygankova OM, Meinkoth JL, Klein PS. Histone deacetylase is a target of valproic acid-mediated cellular differentiation. *Cancer Res*. 2004;64(3):1079–86. <https://doi.org/10.1158/0008-5472>.
 43. Sixto-López Y, Bello M, Correa-Basurto J. Exploring the inhibitory activity of valproic acid against the HDAC family using an MMGBSA approach. *J Comput Aided Mol Des*. 2020;34(8):857–78. <https://doi.org/10.1007/s10822-020-00304-2>.
 44. Zhang H, Penninger JM, Li Y, Zhong N, Slutsky AS. Angiotensin-converting enzyme 2 (ACE2) as a SARS-CoV-2 receptor: molecular mechanisms and potential therapeutic target. *Intensive Care Med*. 2020;46(4):586–90. <https://doi.org/10.1007/s00134-020-05985-9>.
 45. Qin C, Zhou L, Hu Z, Zhang S, Yang S, Tao Y, et al. Dysregulation of immune response in patients with coronavirus 2019 (COVID-19) in Wuhan, China. *Clin Infect Dis*. 2020;71(15):762–8. <https://doi.org/10.1093/cid/cia248>.
 46. Zhang Y, Gao Y, Qiao L, Wang W, Chen D. Inflammatory response cells during acute respiratory distress syndrome in patients with coronavirus disease 2019 (COVID-19). *Ann Intern Med*. 2020;173(5):402–4. <https://doi.org/10.7326/L20-0227>.
 47. Fu B, Xu X, Wei H. Why tocilizumab could be an effective treatment for severe COVID-19? *J Transl Med*. 2020;18(1):164. <https://doi.org/10.1186/s12967-020-02339-3>.
 48. Ichijima T, Okada K, Lipton JM, Matsubara T, Hayashi T, Furukawa S. Sodium valproate inhibits production of TNF- α and IL-6 and activation of NF- κ B. *Brain Res*. 2000;857(1–2):246–51. [https://doi.org/10.1016/S0006-8993\(99\)02439-7](https://doi.org/10.1016/S0006-8993(99)02439-7).
 49. Chen S, Ye J, Chen X, Shi J, Wu W, Lin W, et al. Valproic acid attenuates traumatic spinal cord injury-induced inflammation via STAT1 and NF- κ B pathway dependent of HDAC3. *J Neuroinflammation*. 2018;15(1):150. <https://doi.org/10.1186/s12974-018-1193-6>.
 50. Trougakos IP, Stamatelopoulou K, Terpos E, Tsitsilonis OE, Aivalioti E, Paraskevis D, et al. Insights to SARS-CoV-2 life cycle, pathophysiology, and rationalized treatments that target COVID-19 clinical complications. *J Biomed Sci*. 2021;28(1):9. <https://doi.org/10.1186/s12929-020-00703-5>.
 51. Teodori L, Sestili P, Madiav I, Coppari S, Fraternali D, et al. MicroRNAs bioinformatics analyses identifying HDAC pathway as a putative target for existing anti-COVID-19 therapeutics. *Front Pharmacol*. 2020;11:582003. <https://doi.org/10.3389/fphar.2020.582003>.
 52. Takahashi Y, Hayakawa A, Sano R, Fukuda H, Harada M, Kubo R, et al. Histone deacetylase inhibitors suppress ACE2 and ABO simultaneously, suggesting a preventive potential against COVID-19. *Sci Rep*. 2021;11(1):3379. <https://doi.org/10.1038/s41598-021-82970-2>.
 53. Greer CB, Tanaka Y, Kim YJ, Xie P, Zhang MQ, Park I, et al. Histone deacetylases positively regulate transcription through the elongation machinery. *Cell Rep*. 2015;13(7):1444–55. <https://doi.org/10.1016/j.celrep.2015.10.013>.
 54. Kim YJ, Greer CB, Cecchini KR, Harris LN, Tuck DP, Kim TH. HDAC inhibitors induce transcriptional repression of high copy genes in breast cancer through elongation blockade. *Oncogene*. 2013;32(23):2828–35. <https://doi.org/10.1038/ncr.2013.32>.
 55. Clarke NE, Belyaev ND, Lambert DW, Turner AJ. Epigenetic regulation of angiotensin-converting enzyme 2 (ACE2) by SIRT1 under conditions of cell energy stress. *Clin Sci (Lond)*. 2014;126(7):507–16. <https://doi.org/10.1042/CS20130291>.
 56. Jang I, Kim EN, Lim JH, Kim MY, Ban TH, Yoon HE, et al. Effects of resveratrol on the renin-angiotensin system in the aging kidney. *Nutrients*. 2018;10(11):1741. <https://doi.org/10.3390/nu10111741>.
 57. Lee IH. Mechanisms and disease implications of sirtuin-mediated autophagic regulation. *Exp Mol Med*. 2019;51(9):1–11. <https://doi.org/10.1038/s12276-019-0302-7>.
 58. Bosch-Presegué L, Vaquero A. Sirtuins in stress response: guardians of the genome. *Oncogene*. 2014;33(29):3764–75. <https://doi.org/10.1038/ncr.2013.344>.
 59. Mills RJ, Humphrey SJ, Fortuna PRJ, Lor M, Foster SR, Quafe-Ryan GA, et al. BET inhibition blocks inflammation-induced cardiac dysfunction and SARS-CoV-2 infection. *Cell*. 2021;184(8):2167–218. <https://doi.org/10.1016/j.cell.2021.03.026>.
 60. Yu DC, Waby JS, Chirakkal H, Staton CA, Corfe BM. Butyrate suppresses expression of neuropilin 1 in colorectal cell lines through inhibition of Sp1 transactivation. *Mol Cancer*. 2010;9:276. <https://doi.org/10.1186/1476-4598-9-276>.
 61. Deroanne CF, Bonjean K, Servotte S, Devy L, Colige A, Claussé N, et al. Histone deacetylase inhibitors as anti-angiogenic agents altering vascular endothelial growth factor signaling. *Oncogene*. 2002;21(3):427–36. <https://doi.org/10.1038/sj.onc.1205108>.
 62. Verdecchia P, Cavallini C, Spanevello A, Angeli F. The pivotal link between ACE2 deficiency and SARS-CoV-2 infection. *Eur J Intern Med*. 2020;76:14–20. <https://doi.org/10.1016/j.ejim.2020.04.037>.
 63. Costela-Ruiz VJ, Illescas-Montes R, Puerta-Puerta JM, Ruiz C, Melguizo-Rodríguez L. SARS-CoV-2 infection: the role of cytokines in COVID-19 disease. *Cytokine Growth Factor Rev*. 2020;54:62–75. <https://doi.org/10.1016/j.cytogfr.2020.06.001>.
 64. Mairuae N, Cheepsunthorn P. Valproic acid attenuates nitric oxide and interleukin-1 β production in lipopolysaccharide-stimulated iron-rich microglia. *Biomed Rep*. 2018;8(4):359–64. <https://doi.org/10.3892/br.2018.1062>.
 65. Chen LF, Fischle W, Verdin E, Greene WC. Duration of nuclear NF- κ B action regulated by reversible acetylation. *Science*. 2001;293(5535):1653–7. <https://doi.org/10.1126/science.1062374>.
 66. Chen LF, Mu Y, Greene WC. Acetylation of RelA at discrete sites regulates distinct nuclear functions of NF- κ B. *EMBO J*. 2002;21(23):6539–48. <https://doi.org/10.1093/emboj/cdf660>.
 67. Huang B, Yang XD, Lamb A, Chen LF. Posttranslational modifications of NF- κ B: another layer of regulation for NF- κ B signaling pathway. *Cell Signal*. 2010;22(9):1282–90. <https://doi.org/10.1016/j.cellsig.2010.03.017>.
 68. Perkins ND. Post-translational modifications regulating the activity and function of the nuclear factor kappa B pathway. *Oncogene*. 2006;25(51):6717–30. <https://doi.org/10.1038/sj.onc.1209937>.
 69. Kiernan R, Brès V, Ng RW, Coudart MP, El Messaoudi S, Sardet C, et al. Post-activation turn-off of NF- κ B-dependent transcription is regulated by acetylation of p65. *J Biol Chem*. 2003;278(4):2758–66. <https://doi.org/10.1074/jbc.M209572200>.
 70. Ishinaga H, Jono H, Lim JH, Kweon SM, Xu H, Ha UH, et al. TGF- β induces p65 acetylation to enhance bacteria-induced NF- κ B activation. *EMBO J*. 2007;26(4):1150–62. <https://doi.org/10.1038/sj.emboj.7601546>.
 71. Buerki C, Rothgiesser KM, Valovka T, Owen HR, Rehrauer H, Fey M, et al. Functional relevance of novel p300-mediated lysine 314 and 315 acetylation of RelA/p65. *Nucleic Acids Res*. 2008;36(5):1665–80. <https://doi.org/10.1093/nar/gkn003>.

72. Kodiha M, Salimi A, Wang YM, Stochaj U. Pharmacological AMP kinase activators target the nucleolar organization and control cell proliferation. *PLoS ONE*. 2014;9(1):e88087. <https://doi.org/10.1371/journal.pone.0088087>.
73. Leus NG, van der Wouden PE, van den Bosch T, Hooghiemstra WTR, Ourailidou ME, Kistemaker LE, et al. 3-selective inhibitor RGFP966 demonstrates anti-inflammatory properties in RAW 2647 macrophages and mouse precision-cut lung slices by attenuating NF- κ B p65 transcriptional activity. *Biochem Pharmacol*. 2016;108:58–74. <https://doi.org/10.1016/j.bcp.2016.03.010>.
74. Ji MH, Li GM, Jia M, Zhu SH, Gao DP, Fan YX, et al. Valproic acid attenuates lipopolysaccharide-induced acute lung injury in mice. *Inflammation*. 2013;36(6):1453–9. <https://doi.org/10.1007/s10753-013-9686-z>.
75. Ding D, Greenberg ML. Lithium and valproate decrease the membrane phosphatidylinositol/phosphatidylcholine ratio. *Mol Microbiol*. 2003;47(2):373–81. <https://doi.org/10.1046/j.1365-2958.2003.03284.x>.
76. Xu X, Müller-Taubenberger A, Adley KE, Pawolleck N, Lee VW, Wiedemann C, et al. Attenuation of phospholipid signaling provides a novel mechanism for the action of valproic acid. *Eukaryot Cell*. 2007;6(6):899–906. <https://doi.org/10.1128/EC.00104-06>.
77. Crespillo AJ, Praena B, Bello-Morales R, Lerma L, Vázquez-Calvo A, Martín-Acebes MA, et al. Inhibition of herpes virus infection in oligodendrocyte cultured cells by valproic acid. *Virus Res*. 2016;214:71–9. <https://doi.org/10.1016/j.virusres.2016.01.009>.
78. Pasquereau S, Nehme Z, Haidar Ahmad S, Daouad F, Van Assche J, Wallet C, et al. Resveratrol inhibits HCoV-229E and SARS-CoV-2 coronavirus replication in vitro. *Viruses*. 2021;13(2):354. <https://doi.org/10.3390/v13020354>.
79. Yang M, Wei J, Huang T, Lei L, Shen C, Lai J, et al. Resveratrol inhibits the replication of severe acute respiratory syndrome coronavirus 2 (SARS-CoV-2) in cultured Vero cells. *Phytother Res*. 2021;35(3):1127–9. <https://doi.org/10.1002/ptr.6916>.
80. Stojdl DF, Lichty BD, tenOever BR, Paterson JM, Power AT, Knowles S, et al. VSV strains with defects in their ability to shutdown innate immunity are potent systemic anti-cancer agents. *Cancer Cell*. 2003;4(4):263–75. [https://doi.org/10.1016/s1535-6108\(03\)00241-1](https://doi.org/10.1016/s1535-6108(03)00241-1).

Publisher's Note

Springer Nature remains neutral with regard to jurisdictional claims in published maps and institutional affiliations.

Ready to submit your research? Choose BMC and benefit from:

- fast, convenient online submission
- thorough peer review by experienced researchers in your field
- rapid publication on acceptance
- support for research data, including large and complex data types
- gold Open Access which fosters wider collaboration and increased citations
- maximum visibility for your research: over 100M website views per year

At BMC, research is always in progress.

Learn more biomedcentral.com/submissions

